https://doi.org/10.15407/ufm.19.02.168
PACS numbers: 43.20.+g, 62.20.De, 68.03.Cd, 68.08.Bc, 68.08.De, 68.35.Np, 68.60.Bs, 81.05.Mh, 81.40.Jj, 81.70.Bt

Z. HADEF, A. DOGHMANE, K. KAMLI, and Z. HADJOUB
Laboratoire des Semi-Conducteurs, Département de Physique,
Faculté des Sciences, Université Badji-Mokhtar,
Annaba, BP 12, DZ-23000, Alegria

CORRELATION BETWEEN SURFACE TENSION, WORK OF ADHESION IN LIQUID METALS/CERAMIC SYSTEMS, AND ACOUSTIC PARAMETERS

In the paper, a correlation between acoustic velocities V, elastic moduli M, and densities ρ, with surface tension σ_m, and work of adhesion W_{ad} of different liquid metals on a given ceramic is studied and demonstrated. Simulation program is developed and used for scanning acoustic microscopy (SAM) under operating conditions, which favour the generation of acoustic waves. As found, for the given systems, all investigated acoustic parameters exhibit good dependences with both σ_m and W_{ad}. Analysis and quantification of the results lead to the determination of semi-empirical formulas. The expressions are as follow: $\log(V_i) = 0.49\log(\sigma_m/\rho_{sm}) + B_i$, $M = A_m\sigma_m$, $W_{ad} = C_iV_i$, and $W_{ad} = \xi(M/\rho_{sm})^{1/2} + D_c$, where A_i, B_i, C_i, A_m, ξ, and D_m are characteristic constants for velocities and elastic moduli, the subscripts m relate to the elastic moduli (Young's or shear ones), and $i = L$, T, R — to the propagating longitudinal, transverse, and Rayleigh waves' modes. The importance of the deduced formulas lies in the possibility of prediction of surface tension and work of adhesion of such metal/ceramic interfaces depending on the elastic and acoustic characteristics.

Keywords: surface tension, work of adhesion, acoustic velocities, elastic constants, ceramics, liquid metals, interfaces.

Introduction

The interfacial phenomena between metals and ceramics are one of interest subject in science and engineering. The performance of several technological applications such as ceramic metal bonding, metal–

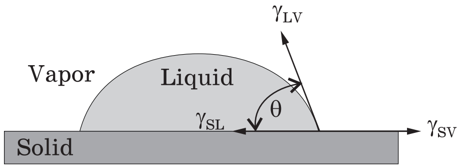

Fig. 1. Contact angle θ in equilibrium liquid/solid system [7]

ceramic joining, ceramic–metal matrix composites [1], thermal-barrier coatings (TBC) [2], hard TiN-coating [3], photovoltaic materials [4], and thin metal films on ceramic substrates [5] is directly linked to the nature of the metal/ceramic interfaces. The behaviour of this interfacial phenomenon is related directly to the nature of interfacial bonding between metal and ceramic [6]. The adhesion of the metal/ceramic system is the most important factor of all metal bonds. It is defined by the change in the free energies of two materials when they come into contact [7].

The work of adhesion W_{ad}, between liquid metal and ceramic substrate is given by Young–Dupré equation relating surface tension of molten metal above melting temperature σ_m and measured equilibrium contact angle θ formed between deposited liquid metal and its ceramic substrate (see Fig. 1) [6]:

$$W_{ad} = \sigma_m(1 + \cos\theta). \tag{1}$$

Various non-destructive techniques are established to characterize the metals-ceramic interfaces [8]. Scanning acoustic microscope (SAM) is one of the important tools for non-destructive determination of adhesion [9]. It can be used quantitatively (microanalysis) and qualitatively (imaging). The microanalysis mode is employed to characterize not only the elastic properties of materials but also the interfacial adhesion *via* propagation of acoustic wave's measurement. It is possible when the interface lies in a plane *xy* and disturbs the propagation of surface acoustic waves (SAWs) [9].

In this paper, a new acoustical approach has been proposed to interpret and estimate the surface tension and work of adhesion in the molten metal/ceramic systems; it shows that these parameters are determined simultaneously *via* acoustic velocities and elastic moduli according to the semi-empirical formulas.

Methodology and Materials

SAM Technique

Scanning acoustic microscope can be applied for a quantitative characterization of the interfacial adhesion *via* the investigation of acoustic material signature, $V(z)$. This analog signal received by transducer and focused by the position of the acoustic lens at the sample against the distance z, under an incidence angle with the reflected ones [10–12]. Its determination based on the calculation of the reflection coefficient $R(\theta)$. The $V(z)$ is the result of the several interferences of all the leaky wave modes, such as leaky SAW, leaky pseudo-SAW, leaky surface-skimming compressional wave, leaky Lamb wave, and harmonic waves. However, only the velocity of leaky SAWs has been extracted from the $V(z)$ curves in microanalysis mode [13]. In effect of the operating conditions of the SAM, only one significant mode dominates all other leaky SAWs modes. Hence, the introduction of fast Fourier transformation (FFT) analysis of $V(z)$ is adopted for the directly determining of the acoustic velocities of materials [13].

V(z) Calculation. The most important quantitative method for elastic parameters determination, in particular, SAW velocities in scanning acoustic microscopy are acoustic material signatures, also known as $V(z)$, which are obtained by recording the output signal, V, as the distance, z, between the sample and the acoustic lens is varied. Such curves, that can be measured experimentally, can also be calculated theoretically, *via* the angular spectrum model [14], from the following expression:

$$V(z) = \int_0^{\theta_{\max}} P^2(\theta) R(\theta) [\exp(2jk_0 z\cos\theta)] \sin\theta\cos\theta\, d\theta. \quad (2)$$

Here, $P(\theta)$ is the distribution function, $k_0 = 2\pi/\lambda$ is the wave number in the coupling liquid, $j^2 = -1$, θ is the angle between the wave vector $\mathbf{k}$ and the lens axis, and $R(\theta)$ is the reflectance function of the specimen. The latter function, for acoustic waves, can be found by solving the acoustic Fresnel equation. The reflection coefficient [15, 16] from a layer reads as

$$R(\theta) = \frac{Z_{in} - Z_{liq}}{Z_{in} + Z_{liq}}, \quad (3)$$

where Z_{liq} is the impedance of plane wave in the liquid, Z_{in} is the input impedance of the layer that is the impedance at the layer–liquid boundary, which is expressed by the formula:

$$Z_{in} = Z_{ch} \frac{Z_{sub} - iZ_{ch}\mathrm{tg}\varphi}{Z_{ch} - iZ_{sub}\mathrm{tg}\varphi} \quad (4)$$

with $\varphi = k_L h_L \cos\theta_L$ being the phase advance of the plane wave passing through the layer of an h thickness, and Z_{sub} and Z_{ch} are the acoustic impedances of substrate and layer given by

$$Z_i = \rho_i V_i / \cos\theta_i, \quad (5)$$

where subscript $i = liq$, ch or sub stands for liquid, layer, or substrate, respectively. It is clear that, at normal incidence, the acoustic impedance becomes simply the product of density and velocity. Hence, the intensity reflection coefficient of a layer on a substrate is as follows:

$$R = \frac{Z_{ch}^2 (Z_{sub} - Z_{liq})^2 \cos^2 k_{ch} h + (Z_{sub} Z_{liq} - Z_{ch}^2)^2 \sin^2 k_{ch} h}{Z_{ch}^2 (Z_{sub} + Z_{liq})^2 \cos^2 k_{ch} h + (Z_{sub} Z_{liq} + Z_{ch}^2)^2 \sin^2 k_{ch} h}.$$

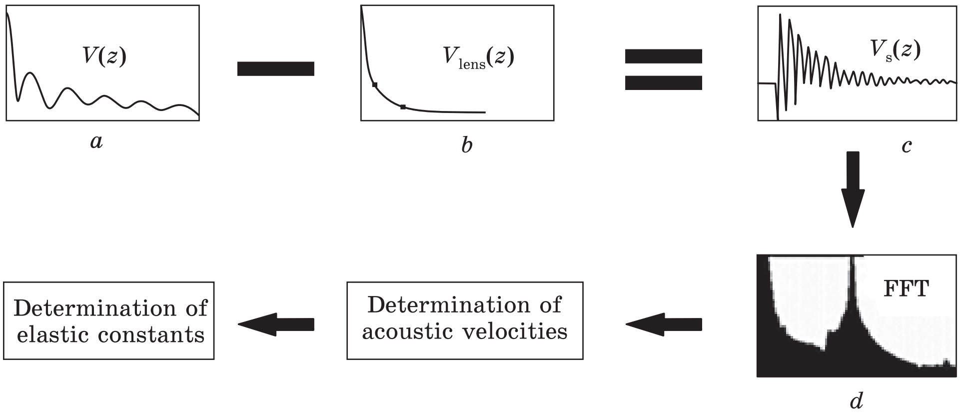

Fig. 2. Schematic diagram showing different calculation steps: *a* — $V(z)$ signature, *b* — lens response, *c* — sample signature, and *d* — spectrum of the fast Fourier transormation (FFT)

Note that the reflection coefficient is a complex-valued function with an amplitude and a phase and the total reflections obtained for $|R(\theta)| = 1$. Therefore, the $V(z)$ calculation from relation (1) can readily be carried out by just knowing the SAW velocities and material densities.

Acoustic Velocity Determination. The schematic representation of $V(z)$ curves, given by Eq. (1), is shown in Fig. 2, *a*; it consists of many peaks and valleys due to constructive and destructive interference between different propagating modes, with a main peak at the focal distance ($z = 0$) representing the lens response. However, successive peaks decay exponentially when z increases, because of the influence of the acoustic lens signal, V_{lens} (Fig. 2, *b*). Thus, the real signal of the specimen, $V_s(z)$, would be

$$V_s(z) = V(z) - V_{lens}(z). \tag{7}$$

Thus, the obtained signal (Fig. 2, *c*) is a periodic curve characterized by a spatial period Δz. Hence, its treatment can be carried out *via* fast Fourier transform (FFT), which exhibits a large spectrum consisting of one or several peaks (Fig. 2, *d*).

The dominant mode (usually Rayleigh one) appears as a very sharp and pronounced peak, from which the Rayleigh velocity can be determined [8] according to the relation:

$$V_R = \frac{V_{liq}}{\sqrt{1 - \left(V_{liq}/(2f\Delta z)\right)^2}}, \tag{8}$$

where V_{liq} is the sound velocity in the coupling liquid and f the operating frequency.

Elastic Constants Determination. It is well known that the Rayleigh velocity is generally determined experimentally from SAM, satisfying the standard equation. In order to determine the elastic constants E and G, Viktorov's formula was used [10]:

$$V_R = V_T \frac{0.718 - (V_T/V_L)^2}{0.75 - (V_T/V_L)^2}.$$

Elastic constants can be expressed in term of density ρ and velocities of the longitudinal V_L and transverse V_T modes of acoustic waves [11].

$$E_1 = \frac{\rho V_T^2[3V_L^2 - 4V_T^2]}{V_L^2 - V_T^2}, \tag{10}$$

$$G_1 = \rho V_T^2. \tag{11}$$

On the other hand, another approach has been proposed [17] to find the relationships between the velocities of the different modes (Rayleigh, longitudinal, and transverse ones) of acoustic waves in order to determine the Young's module E and the shear modulus G by an expression that contains only one of these terms:

$$E_2 = 2.99\rho V_R^2, \tag{12}$$

$$E_2 = 0.757\rho V_L^2, \tag{13}$$

$$E_2 = 2.586\rho V_T^2, \tag{14}$$

$$G_2 = 1.156\rho V_R^2, \tag{15}$$

$$G_2 = 0.293\rho V_L^2. \tag{16}$$

The application of these equations removes several limitations related to SAM operational conditions.

Materials and Simulation Conditions. It is important to note that the determination of Rayleigh velocities of several deposited liquid metals is impossible in using the SAM technique. For this reason, the simulation of deposited metals was taken in a bulk state for determining these Rayleigh velocities, and comparison between obtained results and experimental sound velocities of several deposited liquid metals was made to enrich this study.

The calculations were approved out in case of a reflexion scanning acoustic microscope; Rayleigh mode dominate and appears under normal operating conditions (half-opening angle of lens 50°, working frequency is 142 MHz and water as a coupling liquid whose wave velocity $V_{liq} = 1500$ m/s and density $\rho = 1000$ kg/m^3) or with annular lenses.

The final step consists in determination of the Rayleigh velocities from reflection coefficient and the acoustic signature; for example simulation, it will be taken two metals tin (Sn) and silicon (Si).

Reflection Coefficient. The reflection function, $R(\theta)$, was first calculated for two deposited metals (Sn and Si) to show their effects in the experimental calculation of Rayleigh velocity. The curves obtained are

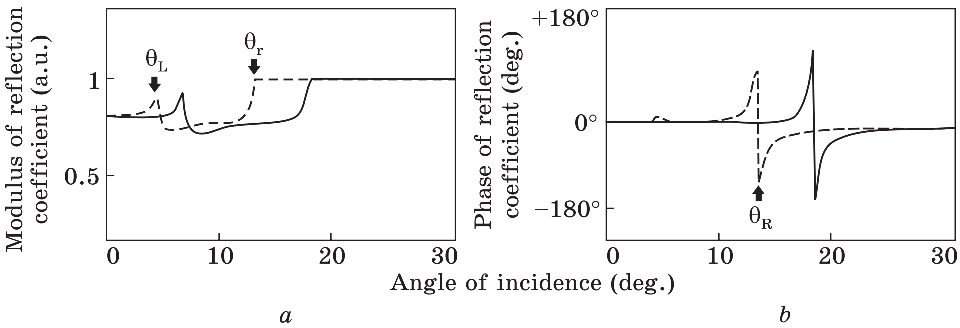

Fig. 3. Reflection coefficients: amplitude (*a*) and phase (*b*) as a function of incidence angles at deposited Sn (dash line) and Si (solid line) metals

shown in Fig. 3. For a better representation of the curve and since $R(\theta)$ is a complex function, we have separated the amplitude curves (Fig. 3, *a*) from those of the phase (Fig. 3, *b*). Then, for the deposited metals mentioned above, the real parts and the imaginary parts were superposed as a function of the angles of incidence θ_i.

Following Fig. 3, *a*, representing the amplitude of $R(\theta)$ as a function of the angle of incidence θ_i, we can clearly observe a first amplitude fluctuation when the angle of incidence reaches the values of the critical longitudinal angles θ_L. A change from θ_L to higher values. Then, a second fluctuation when the angle of incidence reaches the values of the critical transverse angles, θ_T. Between θ_L and θ_T, amplitude of $R(\theta)$ remains constant. Finally, beyond θ_T, the amplitude of $R(\theta)$ increases to reach the unit corresponding to total reflection.

Following Fig. 3, *b*, representing the phase of $R(\theta)$ as a function of θ_I, it can be easily noticed that almost a 2π transition is obtained for Si. This transition occurs at the critical angle, θ_R, which corresponds to the Rayleigh mode, which is the most important in the current simulation conditions. Thus, the Rayleigh mode dominates all other modes leading to the fact that the longitudinal critical angle, θ_L, is not very noticeable.

It can also be seen that the amplitude of the transition in the Rayleigh mode phase becomes lower than the usual 2π value for Sn. While the position, *i.e.* the value of θ_R moves to lower values (similar behaviour to that observed with θ_L in Fig. 3, *a*. In addition, it is clear that all modes are generated with angles less than 20°. These critical angles strongly depend on the simulation conditions, in particular the coupling liquid densities.

Acoustic Signature. The acoustic signature can be calculated from the spectral angular model. The curves obtained for the two deposited metals (Sn and Si), are shown in Fig. 4.

It is clear that the two curves of $V(z)$ exhibit an oscillatory behaviour, with a spatial period Δz, due to constructive and destructive

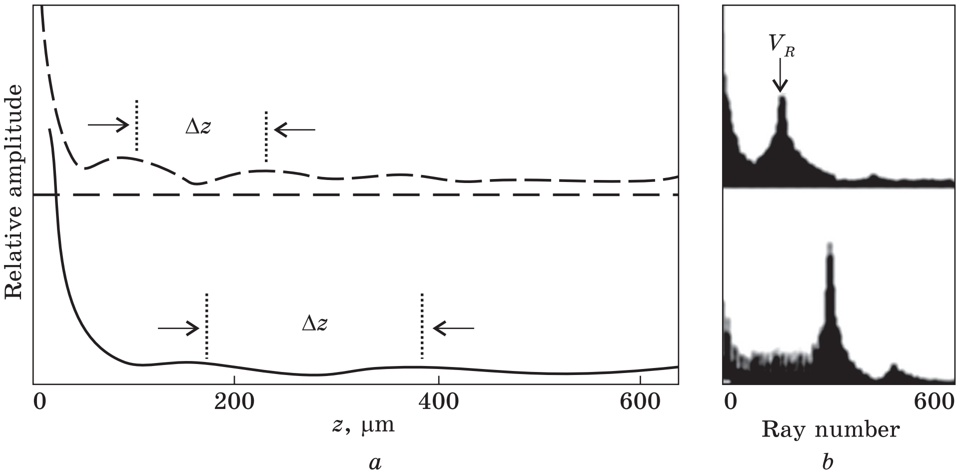

Fig. 4. Acoustic signatures (*a*) and FFT spectra (*b*) for deposited Sn (dash line) and Si (solid line) metals

interferences between the propagation modes. It should be noted that the two curves are distinct in amplitude as well as in the periods, Δz. In amplitudes, the curves attenuate faster for Si corresponding to a large period. Such behaviour is the result of previously observed changes in the module and phase curves of the reflectance functions.

The FFT spectral analysis of these periodic curves $V(z)$ is shown in Fig. 2, *b*. These spectra are characterized by a principal peak representing the most dominant mode, which is that of Rayleigh, under the present conditions. However, the efficiency of this mode represented by its height is more important for higher V_R. Moreover, a small shift is observed for the main ray highlighting the spatial differences Δz obtained in the curves $V(z)$.

Several deposited metals parameters used in this investigation are listed in Table 1; sound velocities at melting temperatures are tabulated by Blairs [18], surface tension values are proposed by Keene [19], liquid densities are taken by Crawley [20] and by Baykara *et al.* [21].While the elastic constants and solid densities are obtained from Briggs [10], Rayleigh velocity determined by SAM and Rayleigh velocity calculated from one-parameter approach are given in Table 1.

Results and Quantification

The objective of this quantification is to find correlations applicable for the estimation of surface tension and the work of adhesion for different liquid metals in contact with ceramic as function of acoustic velocities and elastic constants of these metals.

Table 1. **Experimental sound velocities, c, surface tensions, σ_m, densities, ρ_{lm}, of different liquid metals at the melting temperature, elastic moduli, densities, ρ_{sm}, and calculated Rayleigh velocities, V_R, of these metals at solid state**

Metal	c (m/s)	σ_m (mJ/m^2)	ρ_{lm} (kg/m^3)	E (GPa)	G (GPa)	ρ_{sm} (kg/m^3)	V_R (m/s)	
							SAM	O. P. approach
Na	2526	203	951	10	3.9	968	1720	1875
Mg	4065	577	1589	45	17.4	1738	2879	3078
Al	4561	1075	2390	70	27.1	2700	2929	3130
Si	6920	859	2524	169	18.2	2330	4598	4863
Ca	2978	362	1378	20	7.7	1550	2036	2203
Fe	4200	1909	7042	211	81.6	7874	2806	3003
Co	4031	1928	7740	209	80.8	8900	2808	3005
Ni	4047	1834	7889	207	80.0	8908	2607	2796
Cu	3440	1374	8089	130	50.3	8920	1993	2159
Zn	2850	817	6552	108	41.8	7140	2175	2348
Ge	2693	631	5487	89,6	34.6	5323	2165	2337
Ag	2790	955	9329	83	32.1	10490	1414	1558
Cd	2256	637	7997	50	19.3	8650	1306	1446
Sn	2464	586	6973	50	19.3	7310	1262	1400
Sb	1900	382	6077	55	21.3	6697	1589	1740
Ba	1331	273	3343	13	5.0	3510	1011	1140
La	2030	728	5940	37	14.3	6146	1303	1443
Ce	1694	750	6550	34	13.1	6689	1183	1318
Pr	1926	716	6500	37	14.3	6640	1243	1380
Yb	1274	320	6720	24	9.3	6570	966	1093
Ta	3303	2083	14353	186	71.9	16650	1919	2082
Pt	3053	1746	18909	168	65.0	21090	1574	1724
Au	2568	1162	17346	78	30.2	19300	1008	1136
Sc	4272	939	2680	74	28.6	2985	2841	3039
Ti	4309	1475	4141	116	44.8	4507	2862	3061
V	4255	1856	5340	128	49.5	6110	2641	2831
Y	3258	872	4180	64	24.7	4472	2093	2263
Zr	3648	1463	5650	68	26.3	6511	1846	2006
Nb	3385	1757	7830	105	40.6	8570	1954	2118
Pd	2657	1482	10495	117	45.2	12023	1637	1789
Hf	2559	1517	11550	78	30.2	13310	1361	1503
Nd	2212	685	6890	41	15.9	6800	1272	1411
Sm	1670	431	7420	50	19.3	7353	1359	1501
Eu	1568	264	5130	18	7.0	5244	956	1083
Gd	2041	664	7790	55	21.3	7901	1394	1537
Tb	2014	669	8050	56	21.7	8219	1382	1525
Dy	1941	648	8370	61	23.6	8551	1417	1561
Ho	1919	650	8580	65	25.1	8795	1447	1592
Er	1867	637	8860	70	27.1	9066	1480	1626
Lu	2176	940	9750	69	26.7	9841	1395	1538

Estimation of c and ρ_{lm} in Terms of V_i and ρ_{sm} for Different Solid Metals

In this article, analytical study has been proposed to express the relation between experimental sound velocities of liquid metals at the melting temperature and determinate acoustic velocities of these metals at solid state by SAM program.

It is noted that Rayleigh velocities of bulk metals determined by SAM have almost the same values that these calculated by one parameter approach using Eq. (11).

The variation of V_R values as function of c was made; it shows a linear increase of V_R with c increasing. Simple fitting was made and resulted in a well-defined linear correlation between the quantities, as can be seen in Fig. 5.

The quantified correlation between V_R and c can be written as

$$V_R = 0.674c. \quad (17)$$

Longitudinal and transverse velocities follow similar behaviours that take the following form:

$$V_L = 1.342c, \quad (18)$$

$$V_T = 0.724c. \quad (19)$$

Relation between acoustic velocities of solid metals and experimental sound velocities of liquid metals can be generalized with following analytical form:

$$V_i = A_i c \quad (20)$$

where A_i is a characteristic constant for velocities; the subscripts $i = L$, T, R represent the propagating longitudinal, transverse, and Rayleigh waves modes.

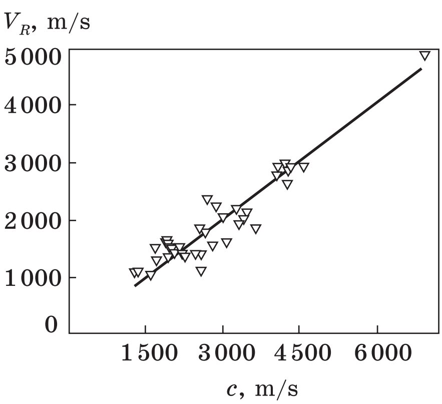

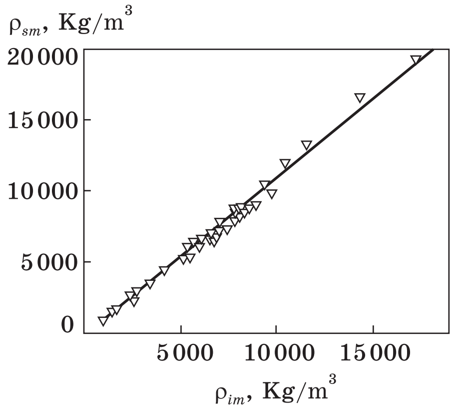

Fig. 5. Correlation between experimental sound velocities c for liquid metals and calculated Rayleigh velocities V_R of these metals in solid state

Fig. 6. Correlation between densities for liquid (ρ_{lm}) and solid (ρ_{sm}) metals

One can see also a clear tendency between the liquid-metals' densities, ρ_{lm}, with that of these metals at solid state, ρ_{sm}, as can be seen in Fig. 6. The relationship that expresses this tendency can take the following form:

$$\rho_{sm} = 1.088\rho_{lm}. \tag{21}$$

The importance of Eqs. (20) and (21) lies in the prediction of acoustic parameters from liquid to solid states of metals and *vice versa*.

Determination of σ_m in Terms of the Acoustic Velocities for Different Metals

Many statistical theories established to associate the surface tension and sound velocities [22–25]. In this context, Auerbach proposed semi-empirical relation to express the sound velocity of such liquid metal at the melting temperature in term of σ_m and ρ_{lm} [26]:

$$c = \sigma_m/6.33\cdot 10^{-10}\rho_{lm}. \tag{22}$$

According to Mayer [27], the previous equation can be written as:

$$c = A(\gamma^{1/2}V_m^{1/6})(\sigma_m/\rho_{lm})^{1/2}, \tag{23}$$

where A is a constant, V_m is the molar volume, and γ is the ratio of the isobaric, C_P, and isochoric, C_V, heat capacities. The plot of $\log(c)$ versus $\log(\sigma_m/\rho_{lm})$ may be linear with a slope equal to 0.67 for Auerbach relation and equal to 0.50 for Mayer relation. This point was study by Blairs [18]; slope equal to 0.552 is found.

In this context, to analyse the functional dependence of σ_m and V_R of solid metals, a linear correlation between the behaviours of quantities is found, where the deduced V_R values increase with increasing of the quantity (σ_m/ρ_{sm}), as can be seen in Fig. 7.

To quantify the relation between V_R and (σ_m/ρ_{sm}), a logarithmic plot was made in the present work; a linear correlation between the quantities is defined by:

$$\log(V_R) = 0.49\log(\sigma_m/\rho_{sm}) + 8.53. \tag{24}$$

It would be noted that similar behaviours were deduced for longitudinal and transverse velocities; this is evident in the following relations:

$$\log(V_L) = 0.49\log(\sigma_m/\rho_{sm}) + 9.22, \tag{25}$$

$$\log(V_T) = 0.49\log(\sigma_m/\rho_{sm}) + 8.60. \tag{26}$$

The above relations of acoustic velocities take the following general form:

$$\log(V_i) = 0.49\log(\sigma_m/\rho_{sm}) + B_i, \tag{27}$$

where B_i is characteristic constants for velocities.

Equation (27) shows that the slope of the plot of $\log(V)$ versus $\log(\sigma_m/\rho_{sm})$ is closer to the Mayer proposition than that of the Auerbach

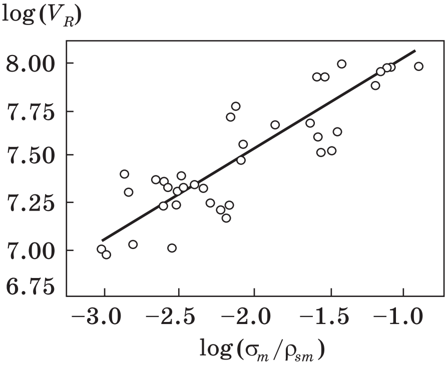

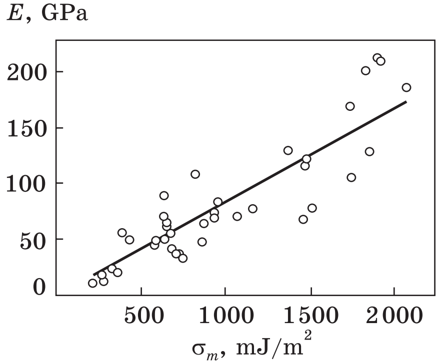

Fig. 7. Correlation between deduced Rayleigh velocities (V_R) and ration of surface tension to density in solid state (σ_m/ρ_{sm})

Fig. 8. Correlation between surface tension σ_m of different liquid metals and Young's modulus E of these metals

relation. It is finds application for the estimation of unknown surface tension of metallic liquids using available acoustic velocities and density values in solid state.

Determination of σ_m in Terms of Elastic Constants for Various Metals

A close comparative of Eqs. (12), (17), and (23) shows a linier dependence between E and σ_m, as can be seen in Fig. 8, where the results' analysis shows increase comportment for surface tension with Young's modulus increasing according to linear relationship; similar behaviour was also obtained for shear modulus.

To quantify the relation between elastic moduli and σ_m, a simple plot was made; a linear correlation is defined that it can be written as

$$E = 0.083\sigma_m, \tag{28}$$

$$G = 0.032\sigma_m. \tag{29}$$

A close comparative analysis of the above equations derived expressions shows that they can be taking the following form:

$$M = A_m\sigma_m, \tag{30}$$

where A_m is characteristic constant for elastic moduli.

An important point that can be interpreted from Eq. (25) is the possibility of determining the unknown surface tension for liquid metals as function of elastic moduli.

Relationship between W_{ad} in Metals/Ceramic Systems and Acoustic Velocities

The principle of the present approach is to find a relation between the acoustic velocities of different metals and the work of adhesion in this several metals on a given ceramic. Experimental results of the work of adhesion and the contact angle for various metal-ceramic systems are summarized in Table 2. It should be taken that the criterion of metal–ceramic systems selected in Tables 2 and 3 is the existence in the literature.

From the plotting of W_{ad} values given in Table 2 against the Rayleigh velocities of the various metals, a linear correlation between these quantities is observed, where W_{ad} increase with V_R increasing as can be seen in Fig. 9 for different metal–aluminium nitride systems.

It is reasonably to express the quantified correlation between W_{ad} and V_R as can be written as

$$W_{ad} = 0.434\,V_R. \tag{31}$$

Table 2. **Experimental values of the work of adhesion W_{ad} for different metal/ceramic systems**

Ceramics	Metal	Atmosphere	W_{ad} (mJ/m^2)	Refs.	Ceramics	Metal	Atmosphere	W_{ad} (mJ/m^2)	Refs.
AlN	Au	Vacuum	550	[28]	BeO	Cu	Ar	600	[31]
	Co	Vacuum	1270	[28]		Fe	He	717	[32]
	Cu	Vacuum	1060	[29]		Ni	Vacuum	680	[32]
	Fe	Vacuum	1320	[28]		Pb	Vacuum	130	[33]
	Ga	Vacuum	750	[28]	BN	Au	Vacuum	205	[34]
	Ge	Vacuum	911	[28]		Cu	Vacuum	345	[34]
	In	Vacuum	448	[28]		Si	Vacuum	664	[34]
	Ni	Vacuum	1305	[28]		Sn	Vacuum	128	[34]
	Pb	Vacuum	203	[28]	MgO	Ag	Ar	421	[34]
	Pd	Vacuum	858	[28]		Fe	Vacuum	820	[35]
	Sn	Vacuum	461	[29]		In	Vacuum	172	[36]
Al_2O_3	Al	Vacuum	948	[30]		Ni	He	585	[37]
	Au	Vacuum	577	[30]		Sn	Vacuum	278	[36]
	Co	Vacuum	1141	[30]	NiO	Ag	Ar	1267	[35]
	Fe	Vacuum	1202	[30]		Cu	Ar	1738	[35]
	Ga	Vacuum	537	[30]		Ni	Ar	2652	[32]
	In	Vacuum	335	[30]		Sn	Vacuum	921	[35]
	Ni	Vacuum	1191	[30]	SiO_2	Au	Vacuum	165	[1]
	Pb	Vacuum	218	[30]		Cu	Vacuum	390	[34]
	Pd	Vacuum	704	[30]		Si	Ar	708	[38]
	Sn	Vacuum	305	[30]					

Table 3. **Slope parameter of Rayleigh velocities, C_R, and the coefficient of the linear regression, R, determined for various ceramic**

Ceramic	C_R	R
AlN	0.434	0.972
Al_2O_3	0.363	0.931
BeO	0.247	0.986
BN	0.137	0.972
MgO	0.236	0.934
NiO	0.859	0.960
SiO_2	0.151	0.976

Similar behaviours of other acoustic velocities would also be deduced; this is evident in the form:

$$W_{ad} = 0.864\,V_L, \tag{32}$$

$$W_{ad} = 0.467\,V_T. \tag{33}$$

The above relations take the following general form:

$$W_{ad} = C_i V_i, \tag{34}$$

where C_i is slope parameter, which gives the interfacial adhesion as function of acoustic velocities.

The points presented in Fig. 9 yields a slope parameter for Al–N. These results, together with the C_R values obtained for other metals–ceramics systems, are given in Table 3.

Moreover, it should be noted that Eq. (34) and C_R values presented in Table 3 determine directly the work of adhesion of different metals–ceramics systems depending on the acoustic proprieties of these metals.

Relation between W_{ad} in Metals/Ceramics Systems and Elastic Constants

To enrich this estimation, it would be useful to quantify the influence of elastic constants on the work of adhesion. The plot of $\log(W_{ad})$ against $\log(E/\rho_{sm})$ is evaluated. Some typical results are summarized in Fig. 10; it is clear that the general tendency is for an increase in W_{ad} as (E/ρ_{lm}) increases.

Using a simple logarithmic plot, it is possible to find linear dependence between logarithms of (E/ρ_{sm}) and W_{ad} as follows:

$$\log(W_{ad}) = 0.504\log(E/\rho_{sm}) - 0.648, \tag{35}$$

$$\log(W_{ad}) = 0.502\log(G/\rho_{sm}) + 2.138. \tag{36}$$

The above elastic moduli (Young's and shear ones) follow similar behaviours, which take the following form:

$$\log(W_{ad}) = 0.502\log(M/\rho_{sm}) + C_m, \tag{37}$$

where C_m is characteristic coefficient for the elastic moduli depending on the nature of ceramic.

This behaviour has been remarked for all ceramics in contact with several liquid metals studied. In this context, a new semi-empirical relation can be proposed to express the work of adhesion in term of E and ρ_{sm} as can be seen in Fig. 11.

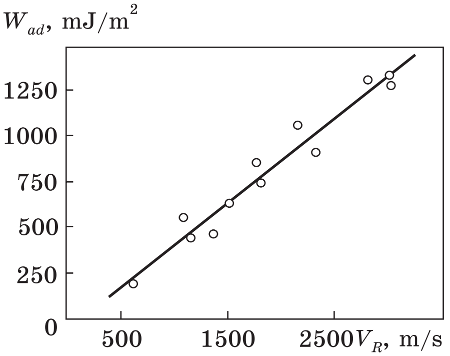

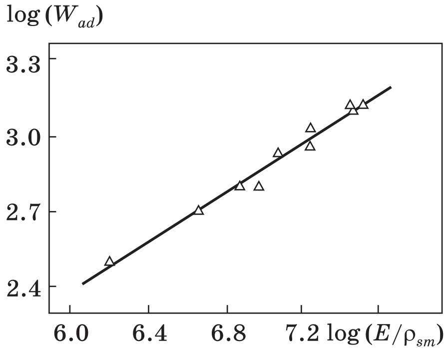

Fig. 9. Correlation between work of adhesion W_{ad} for different metal/AlN systems and Rayleigh velocities V_R of these metals

Fig. 10. Correlation between log(W_{ad}) and log(E/ρ_{sm}) of the metals

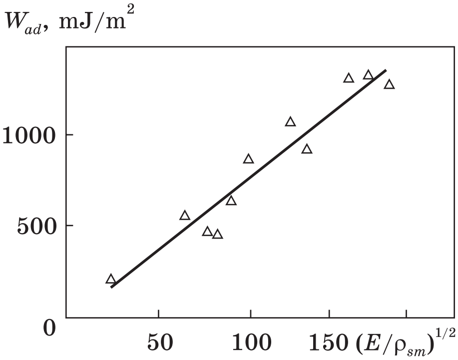

Fig. 11. Correlation between work of adhesion (W_{ad}) of liquid metals/ceramic systems and elastic constant (E/ρ_{sm}) of these metals

Linear correlation between these quantities is defined; it can be written as:

$$W_{ad} = 8.08(E/\rho_{sm})^{1/2} - 41.5, \quad (38)$$

$$W_{ad} = 11.75(E/\rho_{sm})^{1/2} + 52.9. \quad (39)$$

A close comparative analysis of above-mentioned equations derived from expressions shows that they could be taking the following form:

$$W_{ad} = \xi(M/\rho_{sm})^{1/2} + D_c, \quad (40)$$

where ξ represents the slope parameter of dependence on these quantities, and D_C is characteristic coefficient for the elastic moduli depending on the nature of ceramic.

An important point that can be taken from Eq. (40) is the possibility of prediction of work of adhesion in liquid metals/ceramic systems from elastic moduli and densities of liquid metals.

Conclusion

In this work, surface tension and work of adhesion of different liquid metals on a given ceramic are investigated. Acoustic parameters (namely, longitudinal, transverse, and Rayleigh velocities) and elastic constants (namely, Young's and shear moduli) are calculated for all solid metals of the system at issue. It is shown that these parameters change with increasing surface tension as well as with increasing work of adhesion. Applying different complex-quantitative methods [39–43] for the analysis and quantification, we found new linear semi-empirical formulas, which express the variations of velocities and elastic constants. The importance of this estimation consists in the prediction of acoustic parameters for any surface tension and work of adhesion in metals/ceramic interfaces and *vice versa*.

REFERENCES

1. J.G. Li, *Mat. Let.*, **22**, Iss. 3–4: 169 (1995).
2. P.H. Mayrhofer, D. Sonnleitner, M. Bartosik, and D. Holec, *Surf. Coat. Technol.*, **244**: 52 (2014).
3. P. Seiler, M. Baker, and J. Roesler, *J. Comput. Mater. Sci.*, **80**: 27 (2013).
4. N.J. Ekins-Daukes, K.-H. Lee, L. Hirst, A. Chan, M. Führer, J. Adams, B. Browne, K. W.J. Barnham, P. Stavrinou, and J. Connolly, *J. Phys. D: Appl. Phys.*, **46**: 264007 (2013).
5. Y. Imanaka, H. Amada, F. Kumasaka, N. Takahashi, T. Yamasaki, M. Ohfuchi, and C. Kaneta, *Adv. Eng. Mater.*, **15**, No. 11: 1129 (2013).
6. Q. Fu and T. Wagner, *Surf. Sci. Rep.*, **62**, Iss. 11: 431 (2007).
7. G. Triantafyllou and J.T.S. Irvine, *J. Mat. Sci.*, **51**, No. 4: 1766 (2016).
8. A. Kar and A.K. Ray, *Mat. Let.*, **61**, Nos. 14–15: 2982 (2007).
9. B. Cros, M.F. Vallat, and G. Despaux, *Appl. Surf. Sci.*, **126**, Nos. 1–2: 159 (1998).
10. A. Briggs, *Advances in Acoustic Microscopy* (New York: Plenum Press: 1995), vol. **1**.
11. L. Viktorov, *Rayleigh and Lamb Waves* (New York: Plenum Press: 1967).
12. A. Doghmane, S. Douafer, and Z. Hadjoub, *J. Optoelec. Adv. Mat.*, **16**, Nos. 11–12: 1339 (2014).
13. Z. Hadjoub, I. Beldi, and A. Doghmane, *C. R. Phys.*, **8**, Nos. 7–8: 948 (2007).
14. C.G.R. Sheppard and T. Wilson, *Appl. Phys. Lett.*, **38**, No. 11: 858 (1981).
15. L.M. Brekhovskikh, *Wave in Layered Media* (New York: Academic Press: 1980).
16. L.M. Breekhovskikh and O.A. Godin, *Acoustics of Layered Media I* (Berlin: Springer-Verlag: 1990).
17. M. Doghmane, F. Hadjoub, A.Doghmane, and Z. Hadjoub, *Mat. Let.*, **61**, No. 3: 813 (2007).
18. S. Blairs, *J. Coll. Interface Sci.*, **302**, No. 1: 312 (2006).
19. B.J. Keene, *Int. Mat. Rev.*, **38**, No. 4: 157 (1993).
20. A.F. Crawley, *Int. Met. Rev.*, **19**, No. 1: 32 (1974).
21. T. Baykara, R.H. Hauge, N. Noren, P. Lee, and J. L. Margrave, *High Temp. Sci.*, **32**: 113 (1991).

22. P.J. Flory, R.A. Orwall, and A. Vrij, *J. Am. Chem. Soc.*, **86**, No. 17: 3507 (1964).
23. D.J.J. Pandey, *J. Chem. Soc., Faraday Trans. 1*, **76**: 1215 (1980).
24. R.K. Mishra, G. Thomas, and R.L. Mishra, *J. Am. Ceram. Soc.*, **62**, Nos. 5–6: 293 (1979).
25. B.R. Chaturvedi, R.P. Pandey, and J.D. Pandey, *J. Chem. Soc., Faraday Trans. 1*, **78**, No. 4: 1039 (1982).
26. N. Auerbach, *Experientia*, **4**: 473 (1948).
27. S.W. Mayer, *J. Phys. Chem.*, **67**, No. 10: 2160 (1963).
28. N.Y. Taranets and Y.V. Naidich, *Powder Metall. Met. Ceram.*, **35**, Nos. 5–6: 282 (1996).
29. A. Passerone, M.L. Muolo, and F. Valenza, *J. Mater. Eng. Perform.*, **25**, Iss. 8: 3330 (2016).
30. D. Chatain, I. Rivollet, and N. Eustathopoulos, *J. Chem. Phys.*, **83**: 561 (1986).
31. J.G. Li, *Ceramic Int.*, **20**, Iss. 6: 391 (1994).
32. J.G. Li, *J. Am. Ceram. Soc.*, **75**, Iss. 11: 3118 (1992).
33. Ju. V. Naidich, *Progr. Surface Membrane Sci.*, **14**: 353 (1981).
34. M.C. Munoz, S. Gallego, J.I. Beltran, and J. Cerda, *Surf. Sci. Rep.*, **61**, No. 7: 303 (2006).
35. J.G. Li, *Rare Metals*, **12**: 84 (1993).
36. M. Humenik and W.D. Kingery, *J. Am. Ceram. Soc.*, **37**, No. 1: 18 (1954).
37. F.L. Harding and D.R. Rossington, *J. Am. Ceram. Soc.*, **53**, No. 2: 87 (1970).
38. J.G. Li and H. Hausner, *Mat. Let.*, **14**, Nos. 5–6: 329 (1992).
39. V.V. Kurylyak and G.I. Khimicheva, *Usp. Fiz. Met.*, **17**, No. 4: 375 (2016).
40. V.A. Tatarenko, S.M. Bokoch, V.M. Nadutov, T. M. Radchenko, and Y. B. Park, *Defect and Diffusion Forum*, **280–281**: 29 (2008).
41. T.M. Radchenko, V.A. Tatarenko, and S.M. Bokoch, *Metallofiz. Noveishie Tekhnol.*, **28**, No. 12: 1699 (2006).
42. V.A. Tatarenko and T.M. Radchenko, *Intermetallics*, **11**, Nos. 11–12: 1319 (2003).
43. V.V. Kurylyak and G.I. Khimicheva, *Usp. Fiz. Met.*, **18**, No. 2: 155 (2017).

Received May 1, 2018;
in final version, May 3, 2018

З. Хадеф, А. Догман, К. Камлі, З. Хаджуб
Лабораторія напівпровідників, відділ фізики,
факультет наук, Університет Баджі-Мохтара,
Аннаба, БП 12, DZ-23000, Алжир

КОРЕЛЯЦІЯ МІЖ ПОВЕРХНЕВИМ НАТЯГОМ, РОБОТОЮ АДГЕЗІЇ У СИСТЕМАХ РІДКІ МЕТАЛИ/КЕРАМІКА ТА АКУСТИЧНИМИ ПАРАМЕТРАМИ

В статті вперше демонструється кореляція між акустичними швидкостями V, пружніми модулями M, густинами ρ та поверхневим натягом σ_m, а також роботою адгезії W_{ad} різних рідких металів на фіксованій кераміці. Використовується обчислювальна програма для сканувального акустичного мікроскопу (САМ) за умов, що є сприятливими задля ґенерування акустичних хвиль. Виявлено, що для конкретних систем усі досліджені акустичні параметри демонструють хорошу залежність від поверхневого натягу та роботи адгезії. Аналіза та кількісне визначення результатів привели до встановлення напівемпіричних формул. Одержані вирази мають наступний вигляд: $\log(V_i) = 0{,}49\log(\sigma_m/\rho_{sm}) + B_i$, $M = A_m\sigma_m$, $W_{ad} = C_iV_i$ і $W_{ad} = \xi(M/\rho_{sm})^{1/2} + D_c$, де A_i, B_i, C_i, A_m, ξ і D_m є характеристичними значеннями швидкостей і модулів пружности, ніжні індекси m відносяться до модулів пружности (Юнґа чи зсуву), а індекси $i = L$, T, R — до поширюваних поздовжніх, поперечних або Релейових хвиль. Важливість одержаних формул полягає у можливості передбачення поверхневого натягу та роботи адгезії меж поділу метал/кераміка, залежно від пружніх і акустичних характеристик.

Ключові слова: поверхневий натяг, робота адгезії, акустичні швидкості, пружні сталі, кераміка, рідкі метали, межа поділу.

З. Хаэф, А. Догман, К. Камли, З. Хаджуб
Лаборатория полупроводников, отдел физики,
факультет наук, Университет Баджи-Мохтара,
Аннаба, БП 12, DZ-23000, Алжир

КОРРЕЛЯЦИЯ МЕЖДУ ПОВЕРХНОСТНЫМ НАТЯЖЕНИЕМ, РАБОТОЙ АДГЕЗИИ В СИСТЕМАХ ЖИДКИЕ МЕТАЛЛЫ/КЕРАМИКА И АКУСТИЧЕСКИМИ ПАРАМЕТРАМИ

В статье исследуется и впервые демонстрируется корреляция между акустическими скоростями V, упругими модулями M, плотностями ρ и поверхностным натяжением σ_m, а также работой адгезии W_{ad} различных жидких металлов на фиксированной керамике. Используется вычислительная программа для сканирующего акустического микроскопа (САМ) в условиях, благоприятных для генерирования акустических волн. Обнаружено, что для конкретных систем все исследованные акустические параметры демонстрируют хорошую зависимость от поверхностного натяжения и работы адгезии. Анализ и количественное определение результатов привели к установлению полуэмпирических формул. Полученные при этом выражения имеют следующий вид: $\log(V_i) = 0{,}49\log(\sigma_m/\rho_{sm}) + B_i$, $M = A_m\sigma_m$, $W_{ad} = C_iV_i$ и $W_{ad} = \xi(M/\rho_{sm})^{1/2} + D_c$, где A_i, B_i, C_i, A_m, ξ и D_m являются характеристическими значениями скоростей и модулей упругости, нижние индексы m относятся к модулям упругости (Юнга или сдвига), а $i = L$, T, R — к распространяющимся продольным, поперечным или рэлеевским волнам. Важность полученных формул заключается в возможности предсказания поверхностного натяжения и работы адгезии границ раздела метал/керамика в зависимости от упругих и акустических характеристик.

Ключевые слова: поверхностное натяжение, работа адгезии, акустические скорости, упругие постоянные, керамика, жидкие металлы, границы раздела.